Successful observation of orangutans in the wild with thermal-equipped drones

Claire Burke, Maisie F. Rashman, Steven N. Longmore, Owen McAree, Paul Glover-Kapfer, Marc Ancrenaz, and Serge A. Wich

Abstract: We investigated the efficacy of a drone equipped with a thermal camera as a potential survey tool to detect wild Bornean orangutans (*Pongo pygmaeus*) and other tropical primates. Using the thermal camera we successfully detected 41 orangutans and a troop of proboscis monkeys, all of which were confirmed by ground observers. We discuss the potential advantages and limitations of thermal-equipped drones as a tool to complement other methods, and the potential of this technology for use as a future survey tool.

Key words: conservation, UAVs, orangutans, thermal-infrared, sensors.

1. Introduction

Knowledge of the distribution and density of animal species and how these change over time is a key aspect of conservation management and has been achieved by a multitude of ground and aerial based methods (Buckland et al. 2001, 2004; Franklin 2010; MacKenzie 2006). Ground-based surveys (of animals or their signs (e.g. nests, as with orangutans)) (Buckland et al. 2001; Laing et al. 2003; Kühl et al. 2008) are inherently time consuming and can only cover small areas (Ancrenaz et al. 2004). Aerial surveys conducted by manned aircraft can cover larger areas quickly, but are generally costly, are constrained by aircraft availability, and are risky (Wich and Koh 2018; Sasse 2003).

As an alternative and complementary method to manned aerial surveys conservationists are increasingly using drones to monitor animals (Wich and Koh 2018). Detection of animals with drones in open areas has been successful for a number of species from a variety of taxa (review in Wich and Koh 2018), with visible-spectrum cameras used in most cases. Being reliant on reflected sunlight, visible spectrum sensors can only be used during the day, and tend to be ineffective in cases of poor visual

Claire Burke, Maisie F. Rashman, and Steven N. Longmore. Astrophysics Research Institute, LJMU, IC2 Liverpool Science Park, Liverpool, L3 5RF, UK.
Owen McAree. Faculty of Science, Liverpool John Moores University, James Parsons Building, Byrom Street, L3 3AF, Liverpool, UK.
Paul Glover-Kapfer. WWF-UK, The Living Planet Centre, Rufford House, Brewery Rd, Woking, GU21 4LL
Marc Ancrenaz. HUTAN-Kinabatangan Orangutan Conservation Programme, Sandakan, Sabah, Malaysia
Serge A. Wich.[1] School of Natural Sciences and Psychology, Liverpool John Moores University, James Parsons Building, Byrom Street, L3 3AF, Liverpool, UK.
Institute for Biodiversity and Ecosystem Dynamics, University of Amsterdam, Science Park 904, 1098 XH Amsterdam, The Netherlands.

[1]Corresponding author (e-mail: C.Burke@ljmu.ac.uk).

contrast between animals and background, or when animals are located in dense vegetation (Longmore et al. 2017).

Thermal infrared (TIR) sensors offer an advantage over visible spectrum sensors as they detect the light emitted from the animals as a result of their body heat directly. Thus they can be used at night and more effectively through vegetation. Previous studies (Wich and Koh 2018; Chrétien et al. 2015, 2016; Witczuk et al. 2018; Kays et al. 2018) have shown that TIR cameras can indeed be used this way, however they found that thermal radiation emitted by inanimate background features can confound and inhibit animal detection.

We present the results of a pilot study to determine the effectiveness of TIR-equipped drones as a tool to detect and count Bornean orangutans (*Pongo pygmaeus*) and proboscis monkeys (*Nasalis larvatus*) in the wild, and investigate whether these species can be differentiated from each other in TIR data. We discuss the advantages and limitations of this technology as a survey tool to complement other methods.

2. Method

Prior to fieldwork, we developed an observing strategy and rationale to address potential challenges with background temperature and thermal contrast, and determine the minimum apparent size that an animal must appear in the TIR data in order for it to be effectively detected, and hence the maximum drone height above that animal needed to obtain this. Details of the observing strategy and rationale are provided in Appendix A.

Flights were conducted using a Tarot X4 drone with a custom gimbal and a dual thermal-visible spectrum camera. The Thermal Capture Fusion Zoom consists of a 640x512 pixel Flir Tau 2 640 core with a 19mm lens and a 1920x1080 pixel TAMRON visible spectrum (RGB) camera affixed side by side (Appendix A.2).

We conducted 28 flights between 10-15 May 2018 with drone heights between 80–120 m above ground level (AGL). Flights were performed at two sites: Sepilok Orangutan Rehabilitation Centre (SORC) and the Kinabatangan Orangutan Conservation Project (KOCP) (E 118° 17’ 00” to 118° 18’ 40” - N 5° 32’ 20” to 5° 33’ 30”) (Appendix B).

To ensure that we could distinguish the primates from their surroundings, we performed flights before 0900 or after 1900 local time (Appendix A). Researchers with several years of experience examined the TIR data to visually detect the primates (similar to Kays et al. 2018). We determined the robustness of these detections statistically based on the temperature of the entire scene, as detailed in Appendix C.1.

To confirm that the objects detected in the TIR data were indeed orangutans or proboscis monkeys we performed ground confirmation for all potential sightings. This was achieved in two ways. First, a field team was deployed to observe the orangutans and to follow individuals until they nested. The drone was flown to the nesting locations and the footage then inspected visually. Second, a blind drone survey was conducted over a larger area using a grid pattern with 30% image overlap between transects. Following visual inspection the GPS location of any potential detections were recorded and confirmed the next morning if an orangutan or a fresh nest was found at the recorded locations. Fresh nests were identified as having green leaves and the smell of urine/faeces (Appendix A.3).

During our observations at KOCP, we also conducted four flights over proboscis monkeys, which were observed simultaneously from ground level (Appendix B for flight details).

3. Results

Examples of TIR data for our primate detections can be found in the online supplementary materials, and are shown as still frames in appendix D.

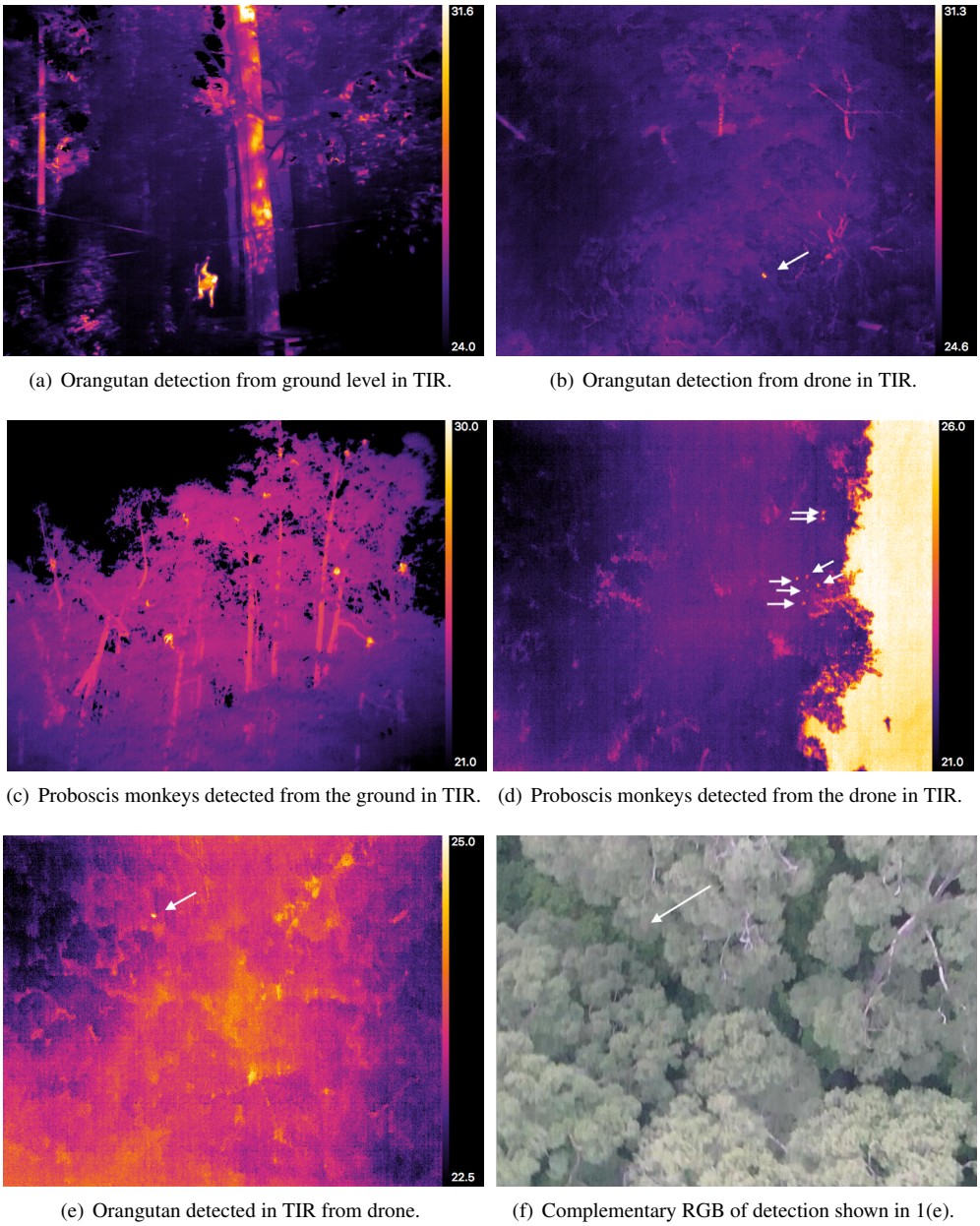

(a) Orangutan detection from ground level in TIR.

(b) Orangutan detection from drone in TIR.

(c) Proboscis monkeys detected from the ground in TIR.

(d) Proboscis monkeys detected from the drone in TIR.

(e) Orangutan detected in TIR from drone.

(f) Complementary RGB of detection shown in 1(e).

Fig. 1. Example of orangutans and proboscis monkeys observed in the TIR data from the ground and drone. The superior capacity to detect primates in TIR imagery compared to RGB imagery is illustrated in the complementary images of the same orangutan shown in frames 1(e) and 1(f).

In total, 28 orangutans that were originally located from the ground were detected in the TIR images from the drone (see figure 1 for examples) – every orangutan found by the ground team was identified in the drone data. Thirteen further detections were made with the blind survey flights and subsequently validated (see table C1 in Appendix B). There were no false positives identified. However, we were

unable to determine the number of false negatives in our data as we did not know the true number of individuals present in the area surveyed.

During four flights we detected a troop of proboscis monkeys (Figure 1), and counted a total of 11 individuals in the group. The troop was also observed from ground level, but the observers were too far away to count numbers with enough reliability to compare with those estimated from the drone data.

We compared the temperature distribution of pixels associated with animal detections to that associated with the environment in the same frames. We found that there was a statistically significant separation between the temperatures of the animals and the surroundings, with no overlap in the two temperature distributions. All orangutans and proboscis monkeys had mean temperatures separated by 4–5 standard deviations from the mean temperature of the surroundings. This is equivalent to a 99.994% – 99.999% confidence of detection (see Appendix C.1).

While relative temperature differences can robustly distinguish orangutan and proboscis monkeys from the background, absolute surface temperatures cannot be used to identify or differentiate different species as animal body temperatures change with that of their environment (McCafferty et al. 2015), as is evident in figure C1. We measured and compared the sizes of the orangutans and proboscis monkeys (figure C2 in Appendix C.1) and found their average sizes to be distinct, in line with the expected difference in size of these animals. However, there was some overlap in size between the largest proboscis monkeys and the smaller orangutans observed, so identification based on size alone is unlikely to be robust. The different behaviour of orangutans and proboscis monkeys, i.e. size of social groups, nesting, is more likely to provide useful information for distinguishing one species from the other. Part of the challenge of species identification is the combination of low resolution cameras with the drone height necessary to avoid trees (in this case). This makes the species of animals detected difficult to discern by eye (discussed in appendix A.1.3).

4. Discussion

Our results indicate that TIR-equipped drones have potential as a tool for detecting primates in a moist tropical rainforest (in line with Kays et al. 2018). During this study we detected 41 orangutans and a troop of proboscis monkeys using this technology and confirmed all TIR detections from the ground.

Using TIR-equipped drones in conjunction with existing survey methods offers several potential advantages. Use of TIR sensors allows surveys to be conducted at times when traditional methods are unusable. Two thirds of our orangutan detections occurred in conditions where the RGB data were unusable and ground surveys would be hindered i.e. at night or during fog. Drones can cover areas more quickly than ground surveys, and at lower cost and risk than manned aircraft. As such, TIR and drone technology together allow animals to be located efficiently for ground follow up and identification.

There are a number of factors to consider and challenges when using this technology. In Appendix A.1.3 we calculated a theoretical maximum distance between the drone and animal of interest for it to be robustly detected, which is 90m for orangutans and 60m for proboscis monkeys. For ground dwelling species this distance informs the maximum drone flying height. However, for arboreal species, a major factor affecting drone flying strategy is canopy height. The canopy height was between $30-50$m and $10-30$m tall for SORC and KOCP respectively, with numerous emergent trees as tall as 65m and 35m, respectively. In an ideal situation the drone would be flown lower than the calculated maximum height to produce data of sufficient resolution for reliable detection and species identification. However, for many of the flights the drone had to be flown higher to safely avoid the emergent trees. As a result, the projected size (in pixels) of the animals in the data was only sufficient for detection, requiring ground follow-up to verify the species. For species identification without a complementary ground survey, possible detections could be immediately confirmed during flight by halting the drone and reducing its height AGL in order to resolve the animal in more detail, then returning to its original height to continue the survey. We are currently developing a fully autonomous on-board system that would allow this procedure to be executed without requiring any intervention by

the ground operators, which will be described in a forthcoming paper.

Previous studies in areas with dense canopy cover have indicated that vegetation can potentially obscure animals in TIR data (Kays et al. 2018; Chrétien et al. 2016). Eleven out of 41 orangutans detected in this study were in nests with $\geq$50% canopy cover, estimated by looking straight up from the position of the nest. Detection of animals with a high percentage of canopy cover may be possible, as the angle at which an animal is viewed will change as a drone passes over. This allows some of the animal's TIR emission to be observed through gaps in the vegetation. However, if an orangutan is 100% obscured from above at all angles by the canopy then it will not be detected. In this case, as has been noted in other studies (Buckland et al. 2004, 2001), there will be a number of individuals which are missed, and the uncertainty of counts will need to reflect this. As we did not know the true number of orangutans in the areas observed in this study, we were unable to estimate the number of false negatives. A detailed investigation into the detection rate of animals using TIR-equipped drones, and how vegetation and other environmental factors impact the detection rate is needed before this technology can be used as a reliable survey tool.

Orangutans occur at low densities, 0.1–4 individuals per km^2 (Husson et al. 2008). Even with a 100% detection rate, large areas would need to be surveyed to estimate orangutan numbers and distribution. Multi-rotor drones are limited by their short battery life, and a typical maximum flight time of 30 minutes, making them unsuitable for large area surveys. Fixed-wing drones are capable of flying for longer and at higher speeds meaning larger distances can be covered. However, they are limited by the requirement for suitable take-off and landing sites.

The necessity for ground-based confirmation of species, as in this study and Kays et al. (2018), remains an unsolved challenge for large area TIR-equipped drone surveys. From our results we suggest that, in its current form, the technology is suitable for surveying species that occur at high densities or range over small areas, where the efficiency of ground surveys will be increased by knowing where animals are located in advance. If an onboard real-time automated detection system such as the one described above could consistently collect sufficiently detailed imagery to confirm primate detections and species, the need for ground validation could be overcome, as well as the requirement for laborious manual analysis of vast extents of imagery over large areas. Given that we have shown that the heat signatures of primates can be robustly distinguished from the background, we believe the data analysis process could indeed be semi-automated, e.g. with machine-learning methods (Longmore et al. 2017; Chrétien et al. 2015, 2016; Lhoest et al. 2015).

In conclusion, in this pilot study we have shown that primates can be detected in tropical rainforests using TIR-equipped drones. At present this technology can be used alongside existing methods to increase the efficacy and efficiency of orangutan surveys. From the observations performed in this study it was only possible to distinguish orangutans from proboscis monkeys based on size. Future studies would benefit from a strategy to improve the spatial resolution of the detections.

Acknowledgements

This work was carried out in partnership with WWF-UK and WWF-Malaysia. We thank the HUTAN-KOCP Orang-utan Research Unit, Sabah Wildlife Department, WWF-UK and WW-Malaysia, Sabah Forestry Department, and Sepilok for their financial and/or logistical support for these tests and granting us permission to do so. We thank Nicola Loweth for facilitating and organising the trip. We also thank Keeyen Pang for conducting the flights. SNL and SW gratefully acknowledge funding from the Research Council UK, Science and Technology Facilities Council grant ST/R002673/1. SNL, SW and CB acknowledge funding from STFC Global Challenges grant ST/P003273/1.

References

Ancrenaz, M., Goossens, B., Gimenez, O., Sawang, A., and Lackman-Ancrenaz, I.: 2004, *Animal Conservation* **7(4)**, 375385

Buckland, S. T., Anderson, D. R., Burnham, K. P., Laake, J. L., Borchers, C. L., and Thomas, L.: 2004, *Advanced Distance Sampling: Estimating Abundance of Biological Populations.*, Oxford University Press.

Buckland, S. T., Anderson, D. R., and Laake, J. L.: 2001, *Introduction to Distance Sampling*, Oxford University Press.

Burke, C., Rashman, M., Wich, S., Symons, A., Theron, C., and Longmore, S.: 2018, *International Journal of Remote Sensing* in press

Chrétien, L.-P., Théau, J., and Menard, P.: 2015, Vol. XL-1/W4

Chrétien, L.-P., Thau, J., and Menard, P.: 2016, *Wildlife Society Bulletin* **40**, 181

Franklin, J.: 2010, *Mapping species distributions: spatial inference and prediction*, Cambridge University Press.

Froehlich, J. W.: 1987, *Journal of Mammalogy* **68(1)**, 200

Husson, S. J., Wich, S. A., Marshall, A. J., Dennis, R. D., Ancrenaz, M., Brassey, R., Gumal, M., Hearn, A. J., Meijaard, E., Simorangkir, T., and Singleton, I.: 2008, *Orangutans: Geographic Variation in Behavioral Ecology and Conservation*, Oxford Scholarship

Kays, R., Sheppard, J., Mclean, K., Welch, C., Paunescu, C., Wang, V., Kravit, G., and Crofoot, M.: 2018, *International Journal of Remote Sensing* pp 1–13

Kühl, H., Maisels, F., Ancrenaz, M., and Williamson, E.: 2008, *Best Practice Guidelines for the Surveys and Monitoring of Great Ape Populations*, Occasional papers of the IUCN Species Survival Commission, World Conservation Union (IUCN) in collab. with the Center for Applied Biodiversity Science

Laing, S. E., Buckland, S. T., Burn, R. W., Lambie, D., and Amphlett, A.: 2003, *Journal of Applied Ecology* **40**, 1102

Lhoest, S., Linchant, J., Quevauvillers, S., Vermeulen, C., and Lejeune, P.: 2015, *The International Archives of Photogrammetry, Remote Sensing and Spatial Information Sciences*

Longmore, S. N., Collins, R. P., Pfeifer, S., Fox, S. E., Mulero-Pazmany, M., Bezombes, F., Goodwin, A., de Juan Ovelar, M., Knapen, J. H., and Wich, S. A.: 2017, *International Journal of Remote Sensing* **38**, 2623

MacKenzie, D.: 2006, *Occupancy estimation and modeling: inferring patterns and dynamics of species occurrence*, Academic Press.

McCafferty, D. J., Gallon, S., and Nord, A.: 2015, *Animal Biotelemetry* **3(1)**, 33

Mittermeier, R. A., Rylands, A. B., and Wilson, D. E.: 2013, *Handbook of the Mammals of the World - Volume 3: Primates*, Lynx Edicions

Sasse, D. B.: 2003, *Wildlife Society Bulletin* **31(4)**, 1015

Wich, S. and Koh, L.: 2018, *Conservation Drones*, Oxford University Press.

Witczuk, J., Pagacz, S., Zmarz, A., and Cypel, M.: 2018, *International Journal of Remote Sensing* **39**, 55035520

A. Detailed Methodology

A.1. Observing Rationale

Prior to all flights in this study, we developed an optimised strategy for observing orangutans and proboscis monkeys following the methods described in Burke et al. 2018.

A.1.1. Flying Times

Successful detection of an object relies on it being distinguishable from its surroundings. In the case of TIR data the distinguishing factor is high thermal contrast - i.e. a large temperature difference between objects of interest and their surrounding environment. To asses the likely thermal contrast between orangutan for our pilot study, we generated a land surface temperature climatology for Sabah during mid-May, Figure A1. The diurnal range for the land surface temperature at this time of year is between $22 - 33°$C. Assuming animals have a fixed temperature, maximum thermal contrast is most likely when the ground is at its minimum temperature. Assuming orangutans have surface temperatures of $\sim 25°$ (see figure 1), observations are most likely to provide successful detections before 09.00 or after 19.00 local time (this is consistent with the findings of Kays et al. 2018).

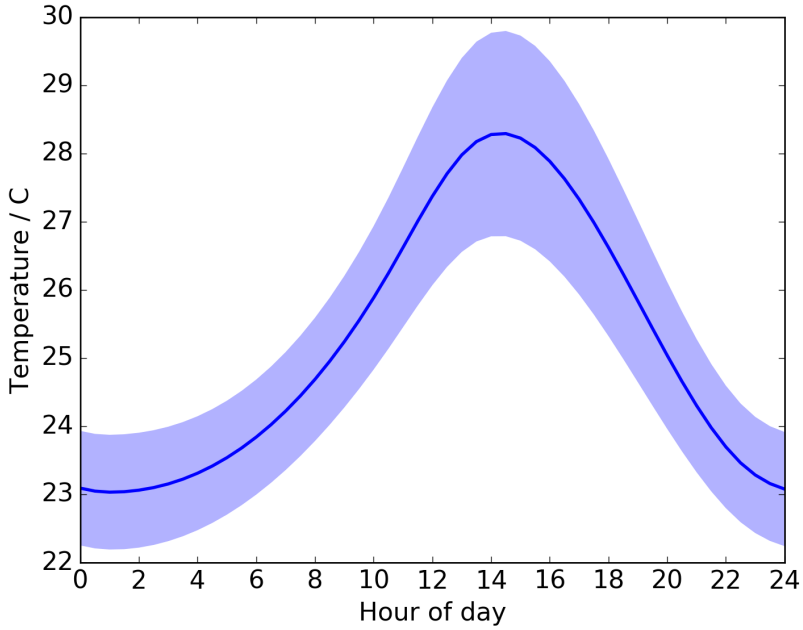

Fig. A1. The average land-surface temperature climatology of a day in mid-May in Sepilok, Sabah, constructed from historical climate observations as described in Burke et al. 2018. The thick line indicates the climatological mean and the shading shows the 2-sigma variation of observed land surface temperature at the Sepilok site.

A.1.2. Weather Conditions

The molecules which make up the atmosphere, like all objects, have an intrinsic temperature. That temperature varies from day-to-day and is often different from the ground temperature. As such the absorption and re-emission of TIR photons by the atmosphere affects the recorded temperature from objects viewed from a distance. Additionally, water vapor is a strong absorber of thermal infrared radiation. It could be expected that the typically humid environment of the Bornean rainforest will affect TIR observations.

Following Burke et al. 2018 we generated absorption spectra for typical weather conditions (temperature, pressure and humidity) in the region, and converted this to a predicted temperature change with distance - Fig A2. From this figure it is clear that for an object with surface temperature 25°C the effect of atmospheric absorption and emission is minimal at flight heights of 120m or lower, and should not significantly impact TIR data collected in this study.

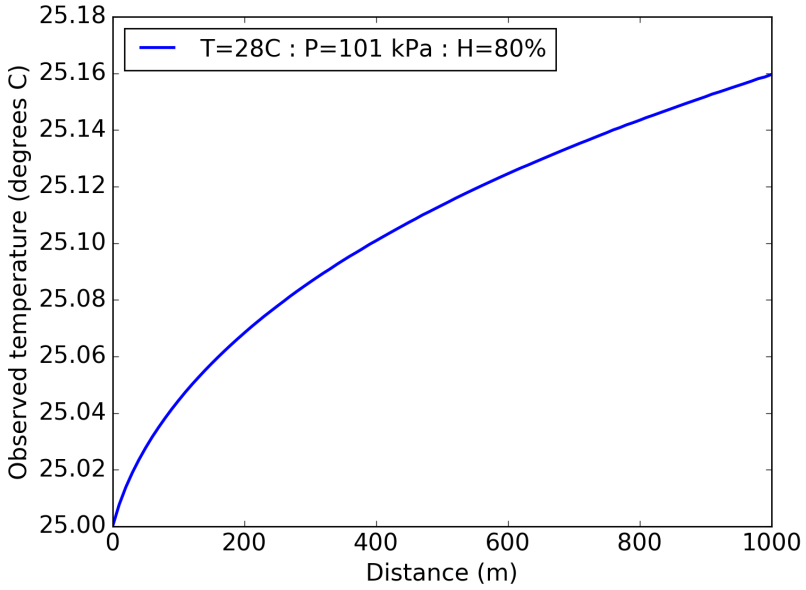

Fig. A2. The temperature which would be observed for an object of 25°C as a result of the typical 28°C air temperature, 80% humidity and 1010hPa pressure expected during May in Sabah. The expected temperature different is negligible.

A.1.3. Flying Height

Given the limited resolution of TIR cameras (640×512 pixels with field of view 32×26° in this case), it is often the case that an individual pixel will contain TIR emission from more than one object. In this study we are concerned about distinguishing between animals and the background. In this case the temperature measured for a single pixel in the TIR camera is a 'blend' of the temperatures of the animal and background imaged within the pixel. As a consequence of this, if the apparent size of an animal is sufficiently small in the field of view (FOV) of the camera, then the temperature of the pixels containing that animal can be significantly different from its true temperature - this is known as the 'spot size effect'. As is shown in Burke et al. (2018), to minimise this effect, the animal of interest must be a minimum of 10 pixels in diameter when viewed by the TIR camera.

This 10 pixel minimum size can be used to set the maximum distance between object of interest and drone by simple geometric relations (see Burke et al. (2018)). Using this we calculated the drone-mounted TIR camera must be flown no higher than $\sim$ 90m above an orangutan, assuming that adult Bornean orangutans are approximately 1.1m in length (Mittermeier et al. 2013). For proboscis monkeys, assuming adults are approximately 0.7m in length (Froehlich 1987), the maximum flying height is $\sim$ 60m (these values can be calculated using the Drone Observing Tool, `http://www.astro.ljmu.ac.uk/~aricburk/uav_calc/`).

A.2. Equipment and Setup

The TeAx Fusion Zoom contains both TIR and RGB (visible spectrum) cameras. The FOV of the RGB and TIR cameras are centered at approximately the same point, with the FOV of the optical camera $\sim$2x larger. Any offset between images from these components can be aligned in post processing. We used a custom built gimbal to decouple the motion of the camera from that of the drone in order to provide a stable platform for data collection. High frequency oscillations are dampened by isolating the entire gimbal mechanism from the airframe by means of a tuned rubber mount. Low frequency dynamics are compensated in both the roll and pitch axis by the presence of a closed-loop brushless stabilisation mechanism which maintains the camera at a constant attitude, independent of the motion of the airframe.

A.3. Flight Strategy

As described above, maximum surface temperatures occur during the day and minimum temperatures at night, making night the preferable observing time for maximum thermal contrast. Due to the need to be able to see the drone for take-off and landing, it was not possible to fly the drone in full darkness, so we performed our flights as close to sunrise ($\sim$06:00) and sunset ($\sim$18:00) as possible. Having some amount of sunlight also meant we were able to gather data with the RGB camera.

Whilst our maximum flying height was set by the calculation described above, in reality other environmental factors influenced our decision on maximum flying height (see section 4). Flights were performed at heights above ground level (AGL) between $30 - 120$m depending on the conditions discussed above. For most flights the camera was pointed straight down during the survey period (90°, nadir position). However, for some flights the camera angle was changed between 45°and 90° during the flight to examine how camera angle affected detectability of animals. Upon visual examination of the TIR data, it was quickly apparent that flying with the camera at 90° made it much easier to detect the orangutans, and no animals were in fact detected with the camera pointed at 45°. All results presented are for the camera pointed at 90°.

The flight pattern selected – grid, line or freestyle – depended on the distance to, and visibility of, the location being surveyed from the take-off site. In general, if the pilot had a line-of-sight view of the GPS position where an orangutan had been seen from the ground, then they flew manually. At larger distances and/or with no direct line-of-sight, the flight was automated following take-off (described in appendix B, also see Table B1). Orangutan nesting sites which were identified during the evening were also surveyed the following morning using the same flight pattern. In SORC orangutan nests were found by following individuals as they left the feeding platform in the rehabilitation centre. In KOCP the Hutan Orangutan field team were observing orangutans as part of ongoing research, and located known individuals and followed these until they nested. The GPS location of nesting sites was recorded and the drone flown to that location. Where distances between the launch site and the nest site were large (> 500m) the drone was flown at a higher height AGL to account for possible changes in terrain height and to give a wider FOV for the camera. As a result, for a small number of flights, the flying height was in the range $80 - 120$m.

B. Detailed flight information

Table B1 describes the details of each flight conducted. Each flight was labelled with a unique Flight ID in the format YYYYMMDD_hhmm. For most flights the height was constant, a small number of flights had varying height and are denoted with an asterisk (*). The majority of flights were conducted at 3 m/s speed, where this value differs it is noted in the table. All recorded values denote the lowest speed travelled during the flight, occasionally a higher speed was used in order to reach the site to be surveyed, and subsequently the speed was decreased whilst covering the area of interest. We surveyed

the nesting sites using 3 different flight patterns; a straight line, a grid (with minimum overlap between transects of 30% of the total FOV) or freestyle, where the pilot manually flew within the line of sight.

Because air temperature, humidity, pressure and wind speed are all environmental conditions which have the potential to affect data quality, we recorded these at ground level with a handheld Kestrel 5500 Weather Meter prior to each flight, Table B2. Temperature, pressure and humidity are not expected to vary significantly over the range of 0-100 m above ground, and small changes in these are not expected to affect data quality as shown in figure A2. The only variable we expect to change noticeably is wind speed. However, this should only have an impact on the stability of the drone and not temperature values recorded.

C. Detailed Results

Table C1 summarised the details of the orangutan detections. Where available, we include information about the canopy coverage and nest height. Knowing the height of both the drone and the nest increases the confidence of detections as we can verify whether the relative size (in pixels) of the object detected falls within the expected size range of orangutans at that height. These quantities were estimated by eye from directly below the nest on the ground, but were not recorded for all ground confirmations. Nest heights were estimated to be between 8 to 20+ m AGL. Since orangutans nest and travel through canopy at varying heights from the ground we believe that the orangutans were closer to the drone than the minimum distance of 90m for most of our flights, and this is supported by the observed nest heights. All potential detections in the TIR data corresponded to the confirmed location of orangutans and/or nests; we directly observed 28 orangutans, and 10 recently vacated nests.

In cases where the drone was flown above 100m AGL, it became noticeably more difficult to detect orangutans. For example, Flight 20180514_1830 (Table C2) was conducted at 120m to survey a large area beyond the visible line of sight of the drone pilot. A mother and infant pair of orangutans had previously been detected and confirmed at this site in flights 20180513_1859, 20180514_0543 and 20180514_0612 (see table C2). One detection was made from the TIR data from flight 20180514_1830, which was verified from the ground the following morning as a recently vacated nest less than 20m above ground level. However, it was noted that the height made the warm spots indicating the presence of an animal particularly difficult to discern. This observation is in line with the expected result of the spot size affect (see A.1.3), and supports the use of a minimum flying height of a drone for observing any animal of interest in order to secure reasonable detections. A minimum height limitation will likely prove challenging for large-area surveys, especially over canopy of unknown topography. For a large area survey, this may be partially circumvented by carrying out a topographical canopy mapping survey beforehand, which will allow drone height to follow that of the canopy for a TIR-equipped drone survey.

Table C2 contains a brief summary of the flights conducted to observe Proboscis Monkeys.

C.1. Statistical differentiation of species based on temperature and sizes

For all frames containing orangutans we constructed histograms of the temperature of pixels containing orangutans and all other pixels within the frame. The orangutan pixels were identified by an algorithm using a temperature threshold. The threshold was set based on the height of the drone AGL, and corresponding expected size of the orangutans in the data. Using an upper limit on the expected size of 1.5 meters, we calculated the percentage of pixels in the FOV that this would cover. This percentage was then used as the percentile threshold for orangutan detection, i.e. the top N% of pixels in the frame were counted as orangutan (or other animal) pixels. The orangutan pixels were then visually confirmed for each frame. The remaining pixels make up the background or surrounding temperature. The temperatures of each pixel extracted this way are shown in figure C1. The same pixels were used to measure the sizes of the orangutans. This was also carried out for data from one flight contain-

Table B1. The details of flights conducted. Launch Site contains information on launch location where Sepilok Orangutan Rehabilitation Centre (SORC) is site A and the lower Kinabatangan-Segama Wetland (KOCP) site is site B. Flying height indicates the maximum height AGL for each flight with a standard error of ± 1 metres. Where flying height was varied this is denoted with an asterisk (*). Flying speed indicated is the minimum for the flight, the estimated uncertainty on this is ±0.1 m/s. Camera angle of 90° denotes the camera pointed straight down (nadir pointing), a forwards slash (/) between two values refers to a change in angle during the flight. Launch times are in local time (Malayisan, MYT). Flight durations were recorded with an accuracy of 0.5 mins. Blue coloured rows highlight flights that were conducted to survey and image proboscis monkeys.

Flight ID (YYYYMMDD_hhmm)	Date (dd/mm/yy)	Launch site	Flying height (m)	Flying speed (m/s)	Camera angle (°)	Launch time	Flight duration (mins)	Flight pattern
20180510_0613	10/05/18	A1	80	-	90	06:13	9	Straight Line
20180510_0622	10/05/18	A1	120	-	90	06:22	7	Straight Line
20180510_0717	10/05/18	A1	120	7	90	07:17	9	Grid
20180510_1824	10/05/18	A2	20*	-	45/90	18:24	11	Freestyle
20180510_1903	10/05/18	A2	120	-	90	19:03	13	Straight Line
20180511_0521	11/05/18	A2	70*	-	45/90	05:21	16	Freestyle
20180511_0528	11/05/18	A1	120	-	90	05:28	5	Straight Line
20180511_0535	11/05/18	A1	100	5	90	05:35	8	Grid
20180511_1744	11/05/18	A1	30*	-	45/90	17:44	4	Freestyle
20180511_1750	11/05/18	A1	30*	-	45/90	17:50	3	Freestyle
20180511_1804	11/05/18	A1	100	1	90	18:04	4	Straight Line
20180511_1830	11/05/18	A1	100	5	90	18:30	10	Grid
20180512_0521	12/05/18	A1	100	-	45/90	05:21	10	Grid
20180512_0541	12/05/18	A1	100	-	45	05:41	10	Grid
20180512_0617	12/05/18	A1	100	1	90	06:17	4	Straight Line
20180512_1804	12/05/18	A1	100	-	90	18:04	12	Freestyle
20180512_1840	12/05/18	A1	76	-	90	18:40	9	Freestyle
20180513_1828	13/05/18	B	80	-	90	18:28	10	Freestyle
20180513_1859	13/05/18	B	80	5	90	18:59	11	Grid
20180514_0543	14/05/18	B	80	5	90	05:43	12	Grid
20180514_0612	14/05/18	B	80	5	45	06:12	12	Grid
20180514_1830	14/05/18	B	120	6	90	18:30	12	Grid
20180514_2020	14/05/18	-	150*	-	45/90	20:20	14	Freestyle
20180515_0512	15/05/18	B	120	6	90	05:12	12	Grid
20180515_0539	15/05/18	B	120	6	90	05:39	4	Grid
20180515_0543	15/05/18	B	100	6	90	05:43	2	Grid
20180515_0545	15/05/18	B	80	6	90	05:45	3	Grid
20180515_0548	15/05/18	B	60	6	90	05:48	5	Grid

ing proboscis monkeys. The histogram of proboscis monkey temperatures is shown in figure C2. A comparison of the sizes of orangutans and proboscis monkeys is shown in figure C2.

For all orangutans and proboscis monkeys there is a distinct gap between their temperature and that of the background. The difference between the mean of each distribution was between 4 and 5 standard

Table B2. The weather data recorded at ground level with a handheld Kestrel 5500 Weather Meter for each flight. Blue coloured rows highlight any flights that were conducted to observe proboscis monkeys. All quoted errors were obtained from the Kestrel 5 series certificate of conformity.

Flight ID	Air temperature (± 0.4 °C)	Humidity (± 1.0%)	Pressure (± 0.3 hPa)	Wind Speed (± 1.66 km/h)
20180510_0613	26.4	83.4	1011.2	1.0
20180510_0622	26.4	83.4	1011.2	1.0
20180510_0717	26.8	80.4	1011.5	2.8
20180510_1824	30.7	76.5	1008.3	0.0
20180510_1903	27.9	89.2	1009.2	0.0
20180511_0521	26.2	83.5	1008.9	1.5
20180511_0528	26.9	85.0	1009.0	0.0
20180511_0535	28.0	82.0	1010.0	0.0
20180511_1744	31.8	73.1	1007.0	0.0
20180511_1750	30.5	75.7	1007.0	0.0
20180511_1804	30.5	75.7	1007.0	0.0
20180511_1830	29.3	84.2	1007.0	0.0
20180512_0521	26.2	79.6	1008.7	0.0
20180512_0541	27.2	88.3	1009.8	0.0
20180512_0617	27.9	84.3	1009.2	0.0
20180512_1804	29.6	85.0	1007.4	1.3
20180512_1840	30.3	74.3	1008.2	1.1
20180513_1828	30.1	75.5	1011.15	1.0
20180513_1859	29.9	79.5	1011.15	1.0
20180514_0543	24.9	82.3	1011.15	1.0
20180514_0612	25.4	90.1	1011.15	1.0
20180514_1830	30.0	81.2	1011.15	1.0
20180514_2020	27.6	81.8	1011.15	1.0
20180515_0512	25.0	84.9	1011.15	1.0
20180515_0539	92.8	83.4	1011.15	1.0
20180515_0543	92.8	83.4	1011.15	1.0
20180515_0545	92.8	83.4	1011.15	1.0
20180515_0548	92.8	83.4	1011.15	1.0

deviations for every orangutan or monkey - equivalent to 99.994% 99.999% confidence of detection.

For the histograms shown in fig C1, two were constructed from morning flights and two were from evening flights. As would be expected from day to day variation in weather and conditions, the temperatures of the background differ between flights performed at the same time of day over the same general area but on different days, and the animals vary their temperature accordingly with the surroundings. As is evident in these figures it is not possible to use absolute temperature for species classification. As is also clear, the shape of distributions changes between flights, times of day, and individuals. From this we conclude that there is not enough consistency between the shape of the

Table C1. Summary of confirmed orangutan sightings from the drone. Orangutan nest heights and canopy cover above the nests are indicated where recorded. The sightings were either orangutans present in their nest, a recently built but vacant nest, or a direct observation of an orangutan not nesting.

Flight ID	Number of detections	Drone height (m)	Nest Height ($\pm$ 2m)	Canopy coverage (%)	Sighting type
Flights at site A					
20180510_0717	1	120	-	-	Nesting orangutan
20180510_1824	1	20	8	75-100	Nesting orangutan
20180510_1903	2	120	-	75-100	2 New nests
20180511_0521	1	70	8	75-100	Nesting orangutan
20180511_0528	1	120	-	75-100	New nest
20180511_0535	2	100	-	-	2 Nesting orangutan
20180511_1744	6	30	-	-	Orangutans observed directly
20180511_1750	6	30	-	-	Orangutans observed directly
20180511_1804	1	100	12	-	New nest
20180511_1830	2	100	-	-	2 Nesting orangutan
	3		-	-	3 Orangutans observed directly
20180512_0521	2	100	>20	0	New nest
			>20	75	New nest
20180512_0541	2	100	>20	0	New nest
			>20	75-100	New nest
20180512_0617	2	100	20	75-100	Nesting mother and infant pair
			<20	50-75	New nest
20180512_1804	3	100	-	-	Moving orangutan
			-	-	Nesting orangutan
			12	0	Nesting orangutan
20180512_1840	1	76	12	0	Nesting orangutan
Flights at site B					
20180513_1859	1	80	<20	75-100	Nesting mother and infant pair
20180514_0543	1	80	<20	75-100	Mother and infant pair
20180514_0612	1	80	<20	75-100	Mother and infant pair
20180514_1830	1	120	<20	-	New nest
20180515_0512	1	120	-	-	Mother and infant pair
Total detections	41				

temperature distributions for orangutans to use it to classify a species from this data. There is also not enough difference between the temperature distribution shapes of orangutans and proboscis monkeys to use this information to tell them apart.

There is a clear difference between the distribution of sizes of the proboscis monkeys and the orangutans. Whilst a small proportion of the proboscis monkey population does overlap with the orangutan distribution, generally the two are distinguishable. Since proboscis monkeys are generally found in groups, whereas orangutans tend to be solitary or in pairs, the combination of size and number of animals seen could be used to distinguish the two. More data and statistical analysis would be needed to understand the possible misclassification rate using this method.

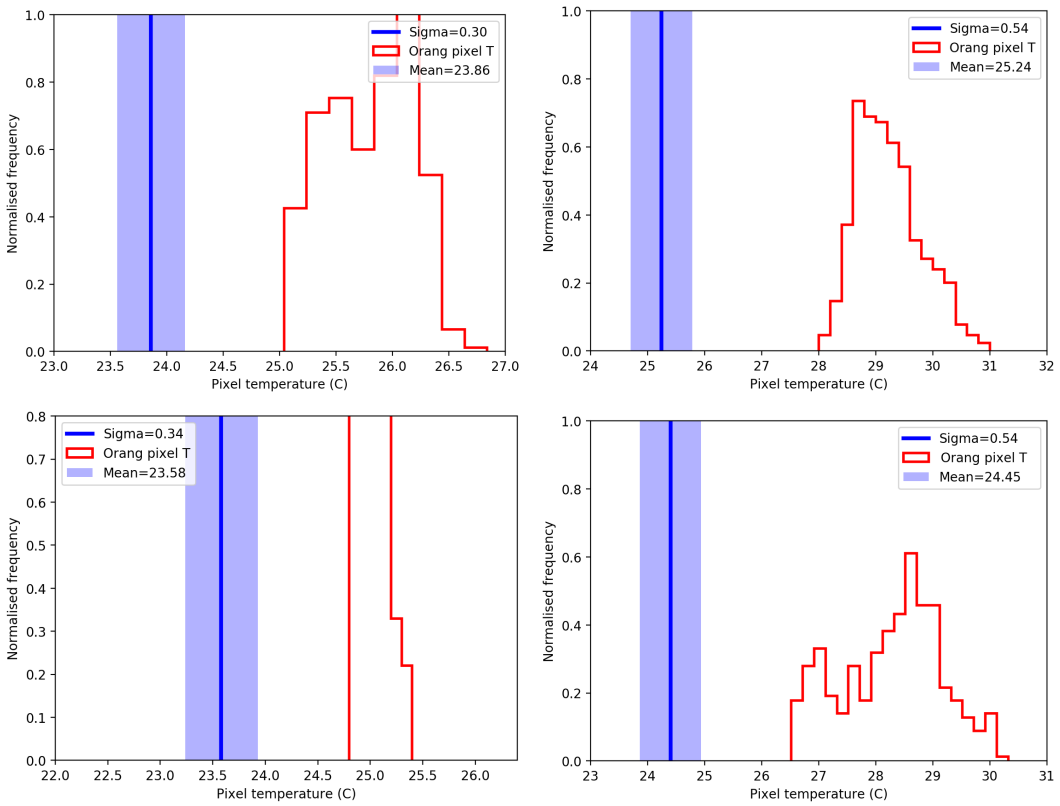

Fig. C1. Examples of temperature distributions of orangutans and their surroundings for 4 flights. Blue line and shading indicates the mean and standard deviation of background pixels respectively. Red histogram indicates the temperature of orangutan pixels. Flight IDs from top left to bottom right: 20180511_0528, 20180511_1830, 20180511_0535, 20180510_1903.

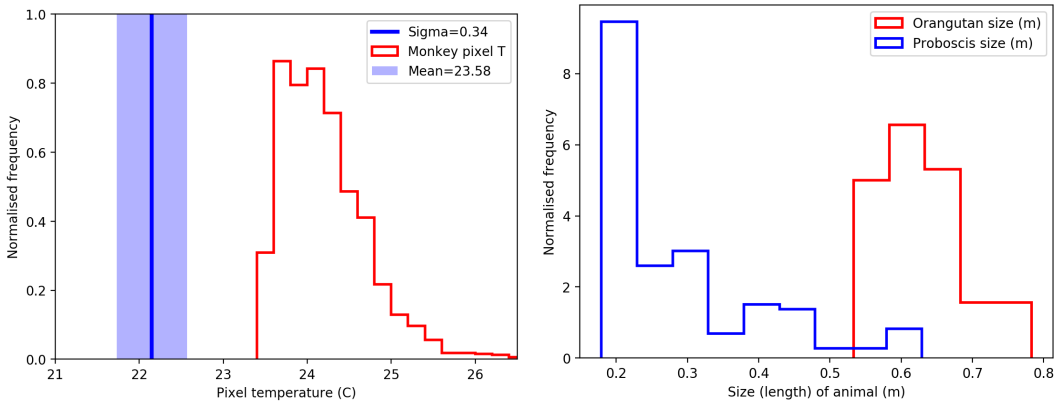

Fig. C2. [Left] Temperature distributions of proboscis monkeys and their surroundings for 1 flight. Blue line and shading indicate the mean and standard deviation of background pixels. Red histogram indicates the temperature of monkey pixels. [Right] Size comparison of orangutans [red] and proboscis monkeys [blue] when viewed from TIR drone images. Flight ID for proboscis monkeys: 20180515_0539.

Table C2. Summary of confirmed proboscis monkey sightings from the drone.

Flight ID	Height	Flight pattern
20180515_0539	120	Grid
20180515_0543	100	Grid
20180515_0545	80	Grid
20180515_0548	60	Grid

C.2. Optical vs thermal infrared detection

Endothermic homeotherms emit most of their energy in the TIR wavelength range (Wein's law). Consequently, animals such as orangutans shine brightly in TIR data, and are particularly visible when their surface temperature is warmer than that of the environment. This is evident in all of our drone observations, where the animals appear as bright objects in the thermal data and are indistinguishable in the RGB (see figures D6–D8 for an example of this).

Being a seasoned observer of orangutans, S.W. attempted to identify orangutans from the optical footage obtained from the drone. This was done in a blind manner, with S.W. having no prior knowledge of where the orangutans had been seen on the ground or in the thermal footage. S.W. found that it was impossible to detect the orangutans with the optical data.

The TIR was also advantageous in conditions where RGB data was unusable - i.e. at night or during fog. In these conditions it would also be difficult or impossible to see the animals from the ground. Figure D23 shows an example of data taken during fog when the optical visibility was estimated by eye from the ground to be only 20m. In this case the orangutans were still clearly visible in the TIR data.

The majority of our 41 TIR orangutan detections came from imaging orangutans in their nests. Orangutans are relatively easy to spot from the ground at this time as they are relatively stationary compared to their active periods during day when they can move quickly through the trees making them particularly difficult to follow on the ground. However nesting times for orangutans are generally when it is dark and they are very difficult to see with an RGB camera or from the ground. Overall we found that TIR extends the times and conditions during which surveys or observations can be conducted into times when optical cameras are unusable and reduced visibility makes ground surveys unsafe. This also makes it possible to increase the detection confidence by observing the same individual nesting in the evening and early the next morning before the nest is vacated.

D. Examples of all primate detections

D.1. SORC Detections

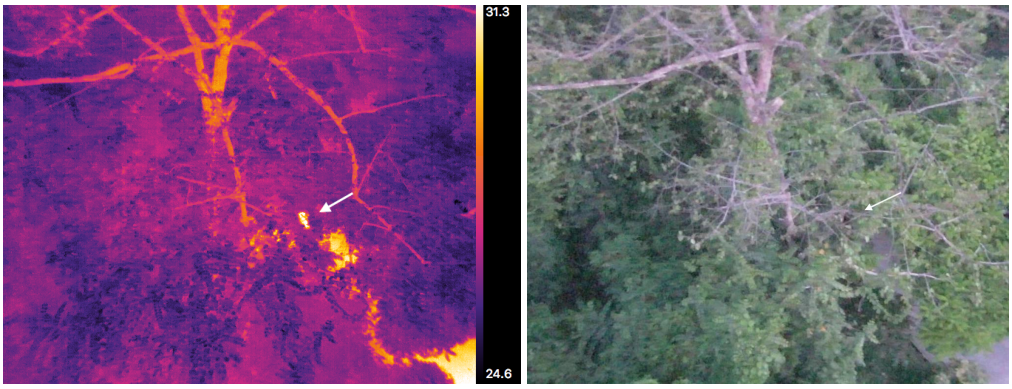

Fig. D1. Confirmed nesting Orangutan detection in Flight 20180510_1824 with camera at 45° in (L) thermal and (R) RGB. Flying height was 20m and canopy coverage was estimated at 75-100%.

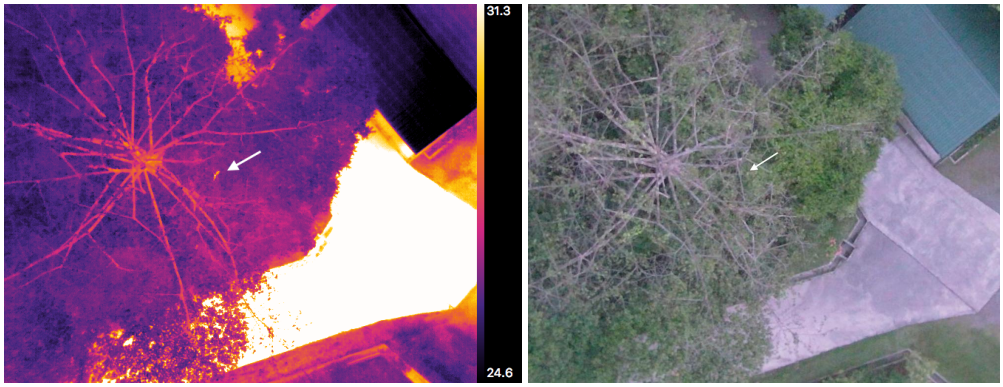

Fig. D2. Confirmed nesting Orangutan detection in Flight 20180510_1824 with camera at 90° in (L) thermal and (R) RGB. Flying height was 20m and canopy coverage was estimated at 75-100%.

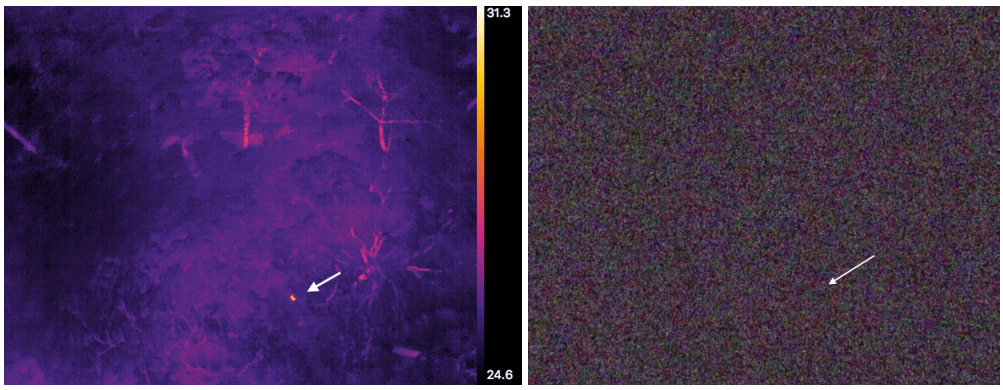

Fig. D3. Confirmed orangutan nest detection in Flight 20180510_1903 in (L) thermal and (R) RGB. Flying height was 120m and canopy coverage was estimated at 75-100%.

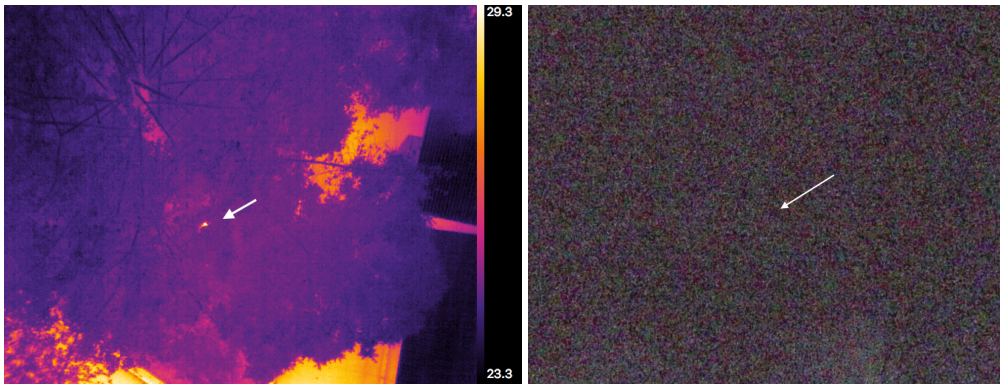

Fig. D4. Confirmed orangutan nest detection in Flight 20180511_0521 in (L) thermal and (R) RGB. Flying height was 70m and canopy coverage was estimated at 75-100%.

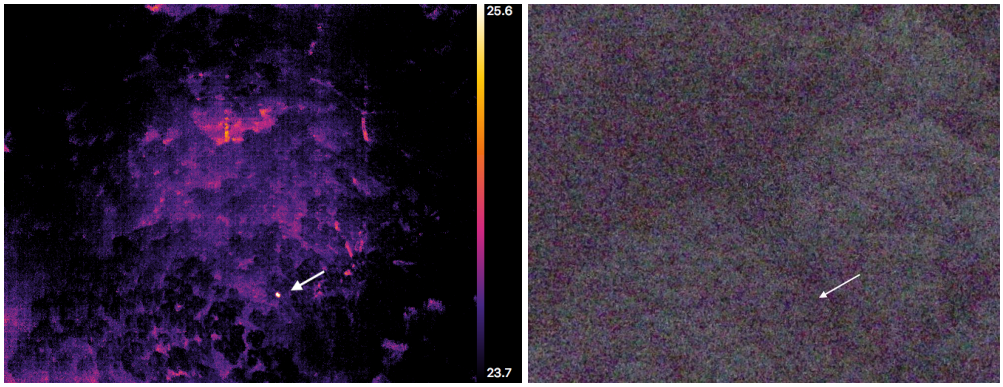

Fig. D5. Confirmed orangutan nest detection in Flight 20180511_0528 in (L) thermal and (R) RGB. Flying height was 120m and canopy coverage was estimated at 75-100%.

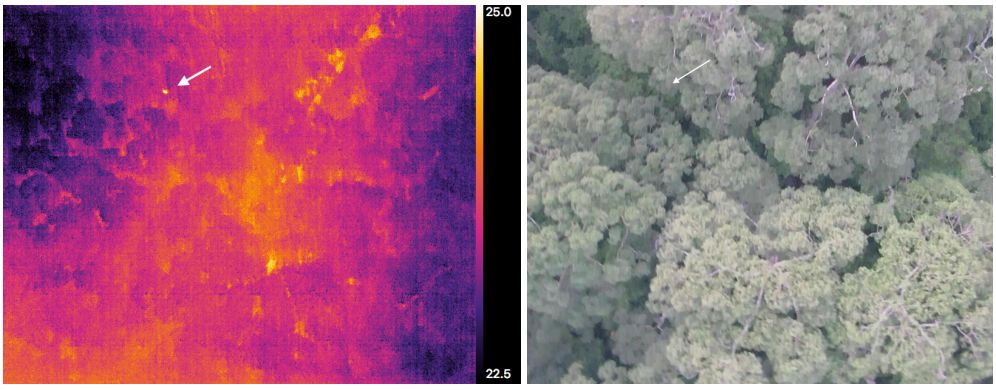

Fig. D6. Confirmed orangutan nest detection in Flight 20180511_0535 in (left) thermal and (right) RGB. Location of orangutan is indicated with an arrow in both images. Flying height was 100m.

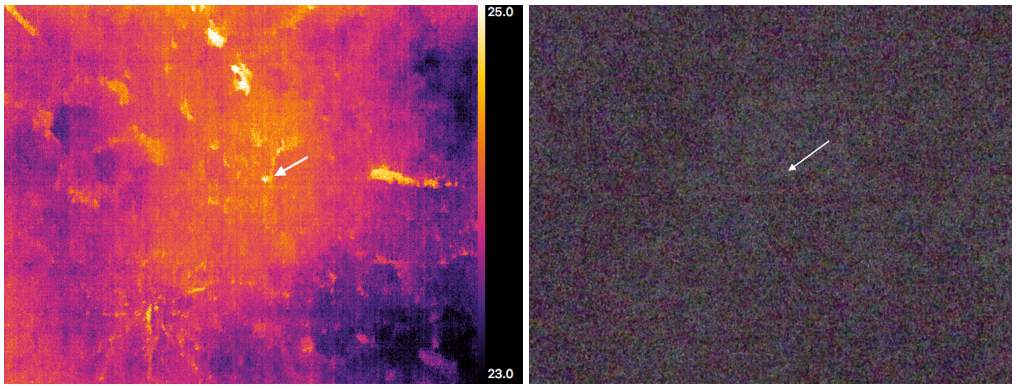

Fig. D7. An example of data from flight 20180512_0521, containing a confirmed detection of a mother and infant orangutan nesting together. Left: TIR image, Right: RGB image. Location of orangutans is indicated with an arrow in both images. This flight was performed just after dawn, making visibility difficult with the RGB. Flying height was 100m and canopy coverage was estimated at 75%.

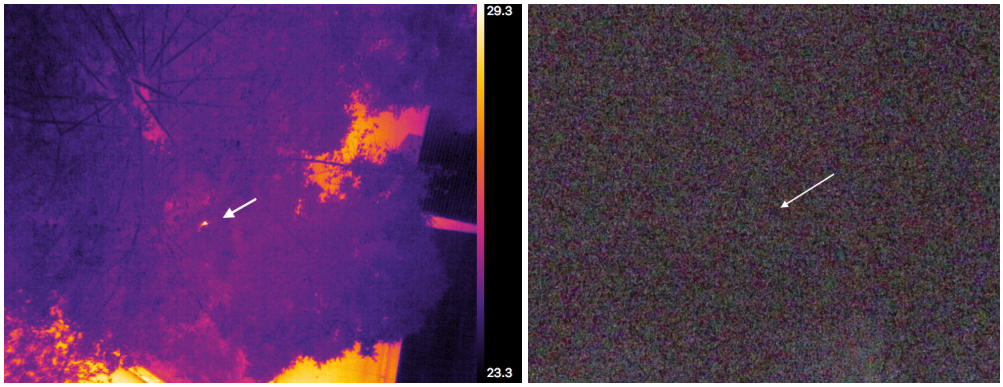

Fig. D8. Confirmed orangutan nest detection in Flight 20180511_0521 in (left) thermal and (right) RGB. This flight was performed just after dawn, making visibility difficult with the RGB. Location of orangutan is indicated with an arrow in both images. Flying height was 100m and canopy coverage was estimated as 0%.

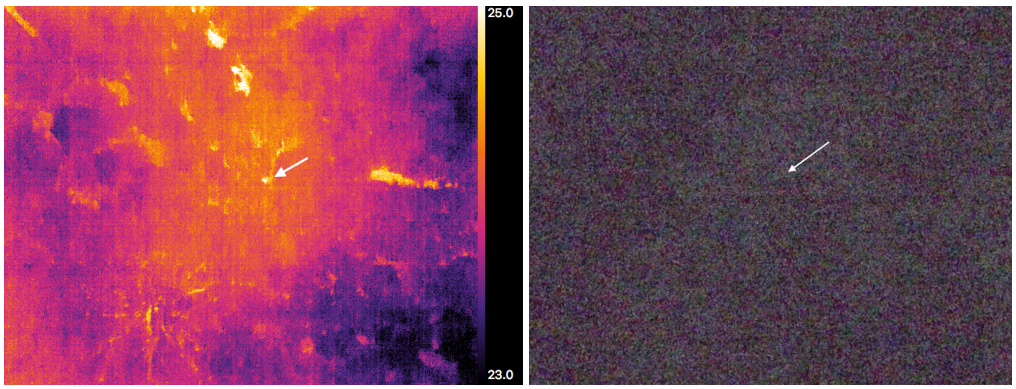

Fig. D9. Confirmed mother and infant pair detected in Flight 20180512_0521 in (L) thermal and (R) RGB. Flying height was 100m and canopy coverage was estimated at 75%.

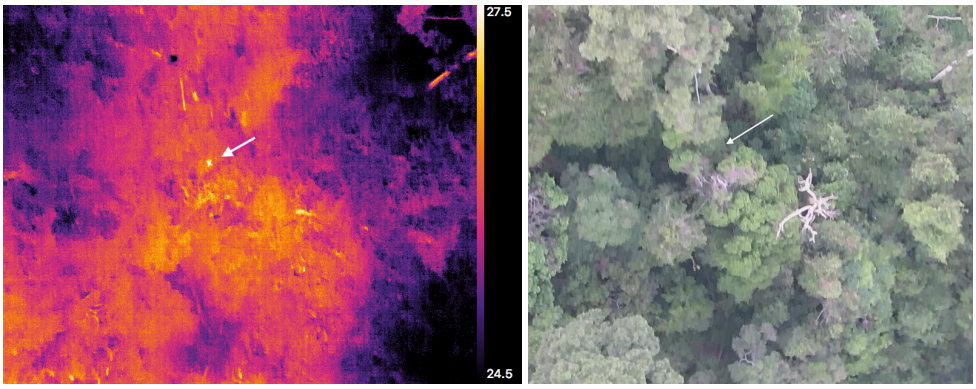

Fig. D10. Confirmed orangutan nest detection in Flight 20180511_1804 in (L) thermal and (R) RGB. Flying height was 100m.

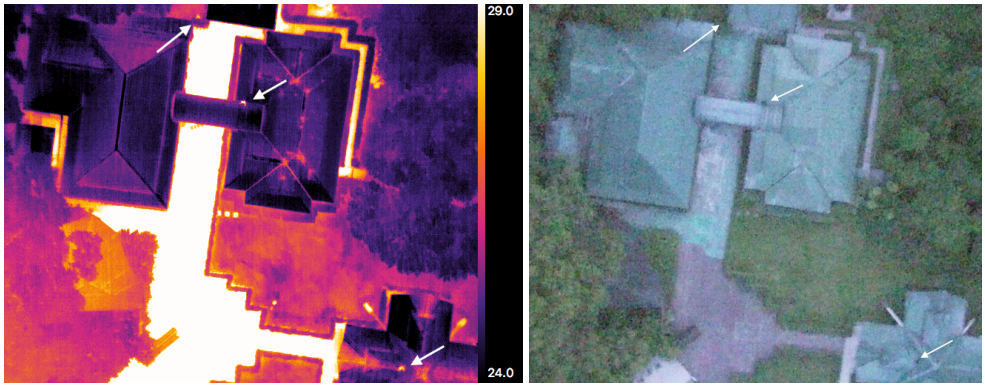

Fig. D11. Confirmed detection of 3 Orangutans on lodge roof in Flight 20180511_1830 in (L) thermal and (R) RGB. Flying height was 100m.

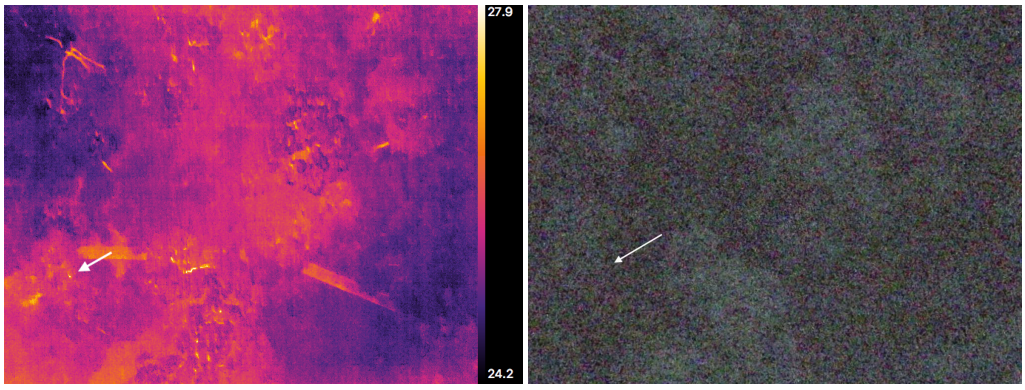

Fig. D12. Confirmed orangutan nest detection in Flight 20180511_1830 in (L) thermal and (R) RGB. Flying height was 100m

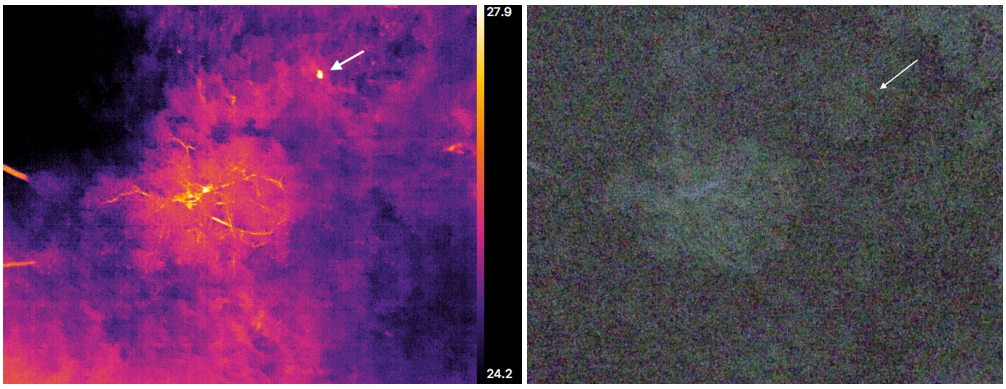

Fig. D13. Confirmed orangutan nest detection in Flight 20180511_1830 in (L) thermal and (R) RGB. Flying height was 100m.

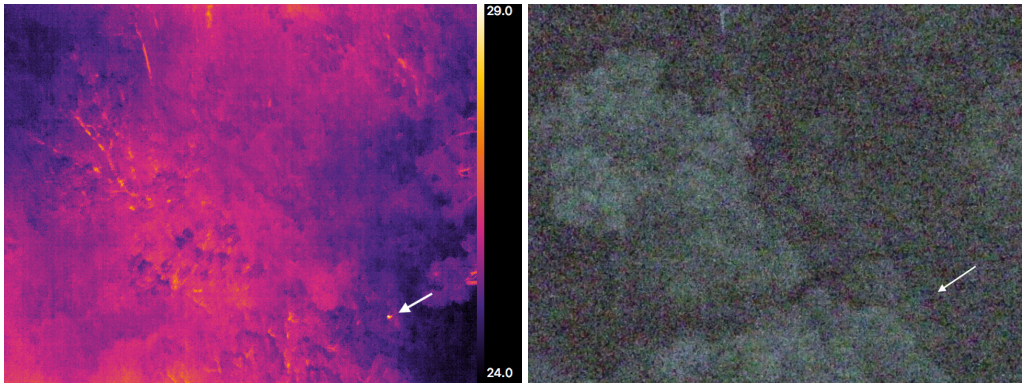

Fig. D14. Confirmed orangutan nest detection in Flight 20180511_1830 in (L) thermal and (R) RGB. Flying height was 100m.

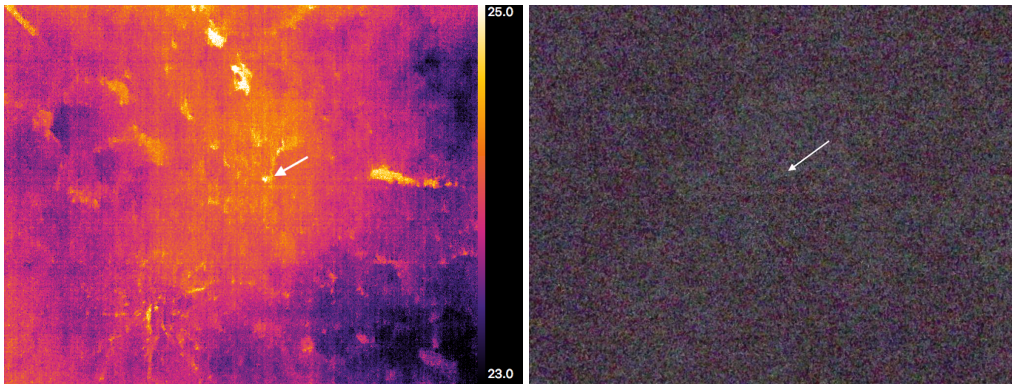

Fig. D15. Confirmed mother and infant pair detected in Flight 20180512_0521 in (L) thermal and (R) RGB. Flying height was 100m and canopy coverage was estimated at 75%.

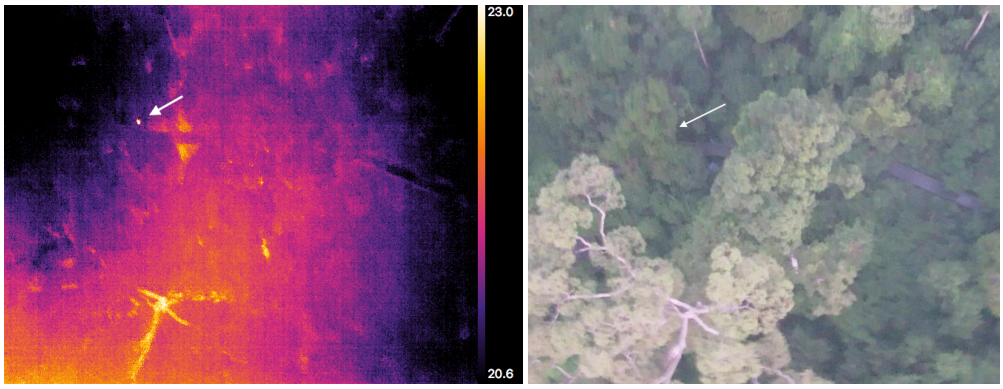

Fig. D16. Confirmed orangutan nest detection in Flight 20180512_0541 in (L) thermal and (R) RGB. Flying height was 100m and canopy coverage was estimated at 75-100%.

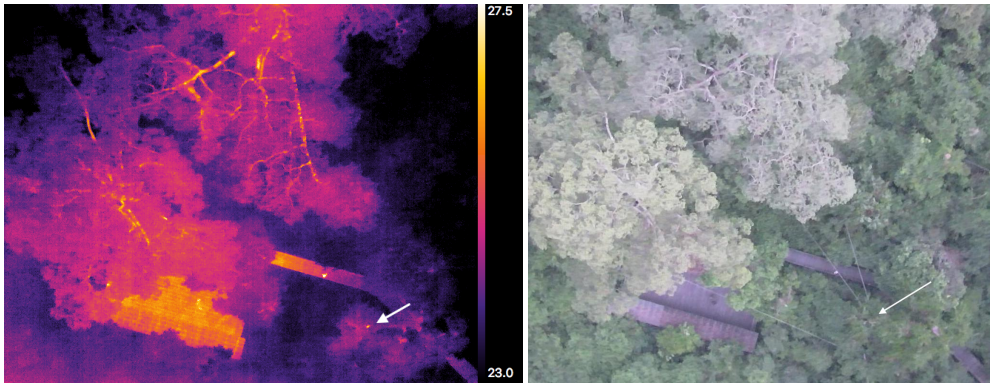

Fig. D17. Confirmed orangutan nest detection in Flight 20180512_1804 in (L) thermal and (R) RGB. Flying height was 100m.

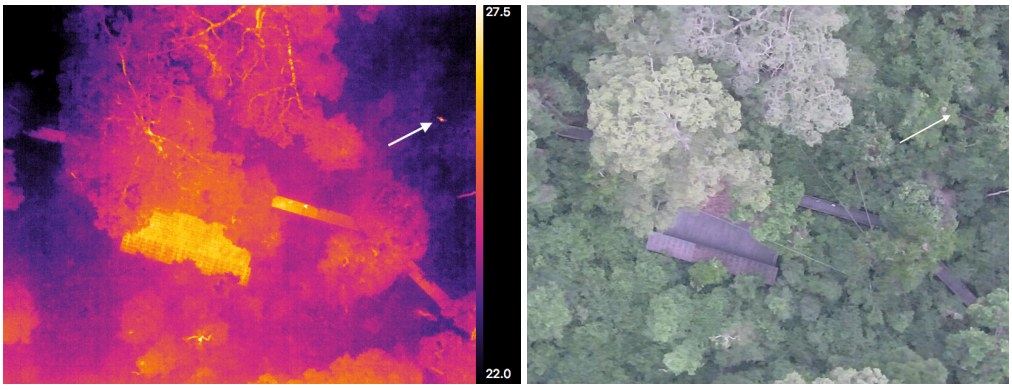

Fig. D18. Confirmed moving orangutan detection in Flight 20180512_1804 in (L) thermal and (R) RGB. Flying height was 100m.

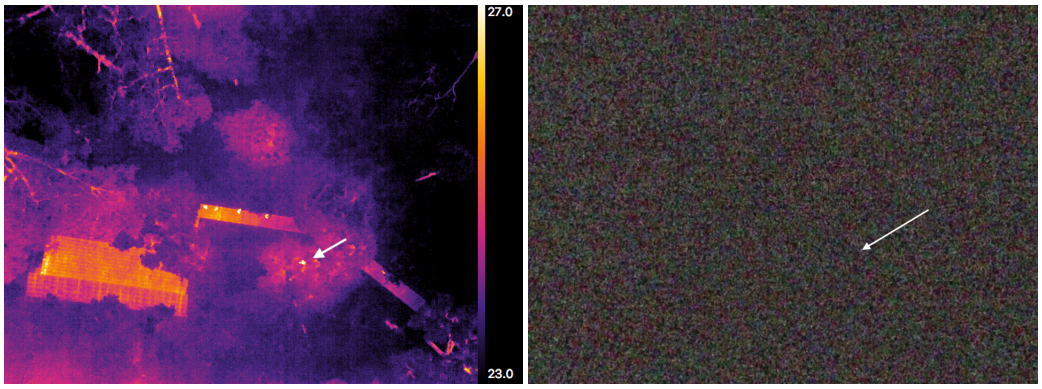

Fig. D19. Confirmed orangutan nest detection in Flight 20180512_1804 in (L) thermal and (R) RGB. Flying height was 100m and canopy coverage was estimated at 0%.

335 ## D.2. KOCP Detections

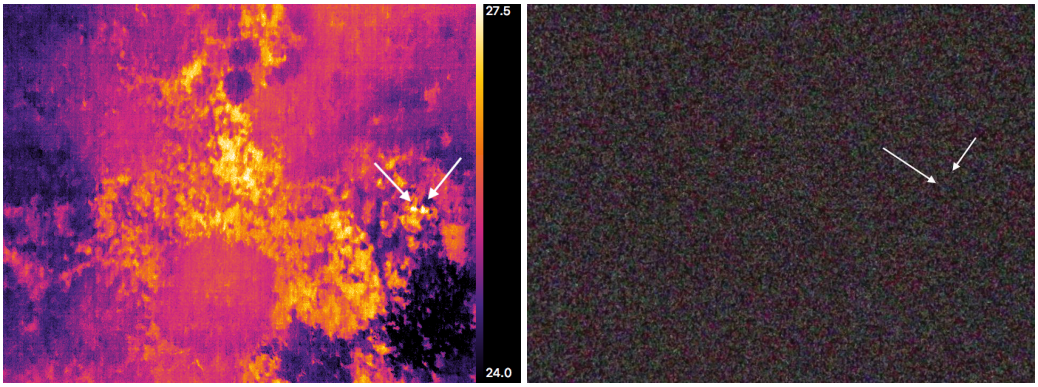

Fig. D20. Confirmed orangutan nest detection in Flight 20180513_1859 in (L) thermal and (R) RGB. Flying height was 80m and canopy coverage was estimated at 75-100%.

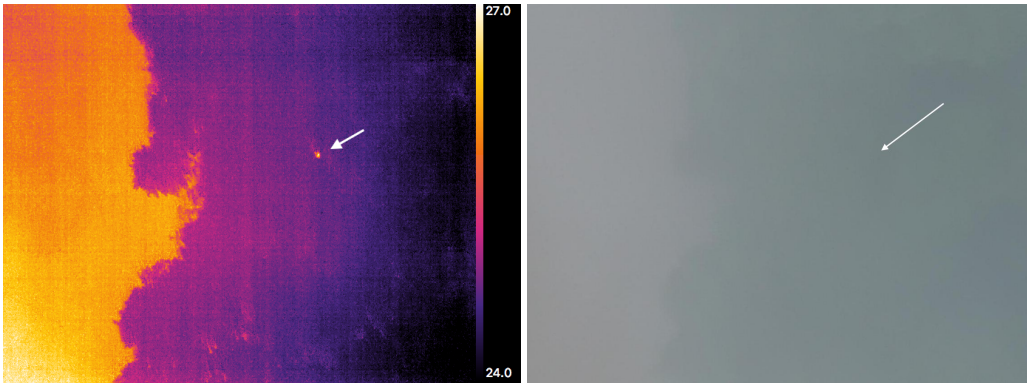

Fig. D21. Confirmed orangutan nest detection in Flight 20180514_0543 in (L) thermal and (R) RGB. Flying height was 80m and canopy coverage was estimated at 75-100%.

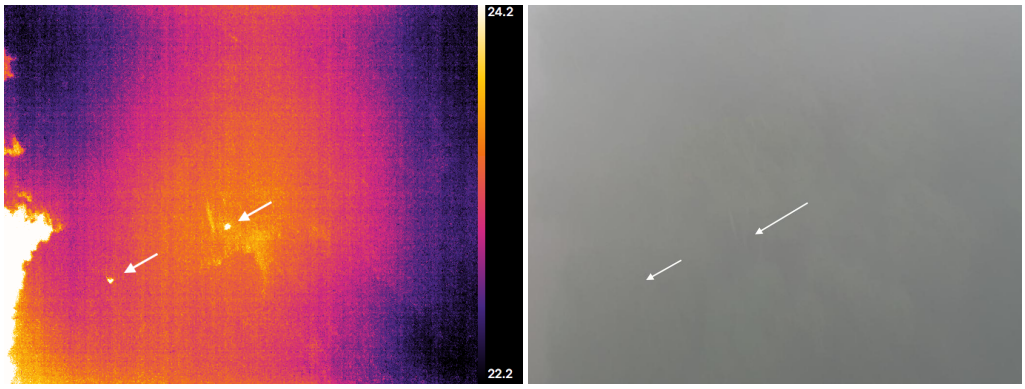

Fig. D22. Confirmed mother and infant pair detected in Flight 20180514_1612 in (L) thermal and (R) RGB. Flying height was 80m and canopy coverage was estimated at 75-100%.

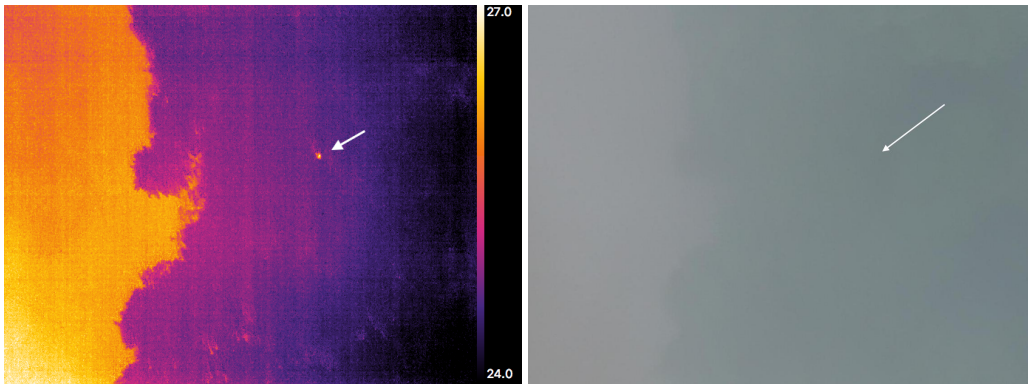

Fig. D23. Confirmed orangutan nest detection in Flight 20180514_0543 in (left) thermal and (right) RGB. This flight was performed under foggy conditions, with visibility from the ground $<$ 20m by eye. Location of orangutan is indicated with an arrow in both images. Flying height was 80m and canopy coverage was estimated at 75-100%.

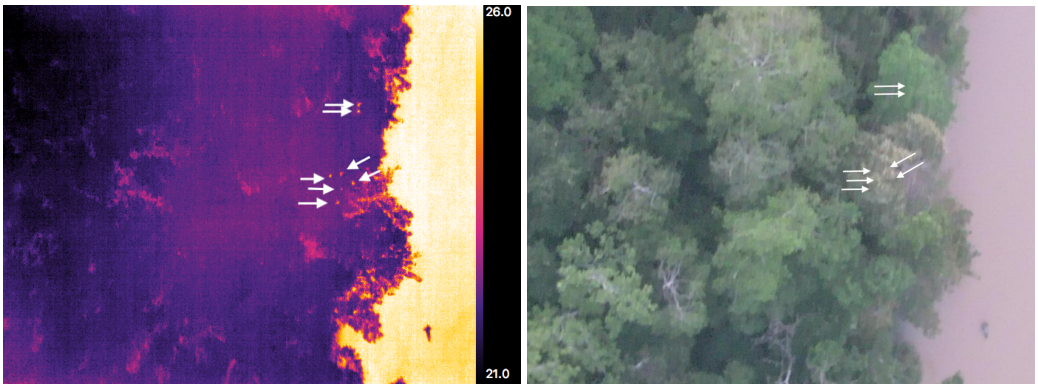

Fig. D24. Proboscis monkeys from drone at 100m with thermal camera (left) and RGB camera (right).